

Color Octet Electron Search Potential of the FCC Based e-p Colliders

Y. C. Acar

*Department of Electrical and Electronics Engineering,
TOBB University of Economics and Technology, Ankara, Turkey**

U. Kaya

*Department of Material Science and Nanotechnology,
TOBB University of Economics and Technology, Ankara, Turkey and
Department of Physics, Faculty of Sciences, Ankara University, Ankara, Turkey†*

B. B. Oner

*Department of Material Science and Nanotechnology,
TOBB University of Economics and Technology, Ankara, Turkey*

S. Sultansoy

*Department of Material Science and Nanotechnology,
TOBB University of Economics and Technology, Ankara, Turkey and
ANAS Institute of Physics, Baku, Azerbaijan‡*

Resonant production of color octet electron, e_8 , at the FCC based ep colliders has been analyzed. It is shown that e-FCC will cover much a wider region of e_8 masses compared to the LHC. Moreover, with highest electron beam energy, e_8 search potential of the e-FCC exceeds that of FCC pp collider. If e_8 is discovered earlier by the FCC pp collider, e-FCC will give opportunity to handle very important additional information. For example, compositeness scale can be probed up to hundreds TeV region.

arXiv:1605.08028v4 [hep-ph] 31 Oct 2016

* ycacar@etu.edu.tr

† ukaya@etu.edu.tr

‡ ssultansoy@etu.edu.tr

I. INTRODUCTION

Standard Model (SM) has proven its reliability by the experimental verifications of its particle content in the recent decades. SM puzzle has been completed by the discovery of Higgs boson [1, 2]. However, SM seems not to be the end of the whole story. There are still many unsolved problems that are out of the scope of the SM and especially the large number of currently known elementary particles becomes more of an issue. For this reason a lot of BSM models have been proposed including extension of scalar and fermionic sectors of SM, enlargement of SM gauge symmetry group, SUSY, compositeness (preons [3]), extra dimensions etc. Keeping in mind historical development of fundamental building blocks of matter, the search for preonic models seem to be quite natural. This development is summarized in Table I.

Table I. Historical development of fundamentality.

Stages	1870-1930s	1950-1970s	1970-2030s
Fundamental Constituent Inflation	Chemical Elements	Hadrons	Quarks, Leptons
Systematics	Periodic Table	Eight-fold way	Family Replication
Confirmed Predictions	New Elements	New Hadrons	BSM particles
Clarifying Experiments	Rutherford	SLAC-DIS	LHC or rather FCC?
Building Blocks	Proton, Neutron, Electron	Quarks	Preons?
Energy Scale	MeV	GeV	TeV?
Impact on Technology	Exceptional	Indirect	Exceptional

Family replication and especially SM fermion mixings can be considered as indications of preonic structure of matter. One of the notable results of preonic models is prediction of well-known BSM particles (such as excited leptons and quarks, leptoquarks) and contact interactions which are widely investigated by ATLAS and CMS. In composite models with colored preons (see [4] and references therein), leptons have color octet partners, ℓ_8 , which are known as leptogluons. Phenomenologically their status is similar to excited leptons and leptoquarks. Experimentally excited leptons and leptoquarks are considered in CMS and ATLAS experiment searches, however, there is no direct search on leptogluons.

There are a number of phenomenological studies on ℓ_8 production at TeV colliders. For example, production of leptogluons at the LHC has been analyzed in [5–9]. Resonant production of leptogluons at ep and μp colliders were considered in [10–12] and [13], respectively. Indirect production of leptogluons at ILC and CLIC has been studied in [14]. On the other hand, considering IceCube PeV events [15], color octet neutrinos may be source of these extraordinary events [16].

Experimental bound on color octet electron (e_8), $M_{e_8} > 86 \text{ GeV}$, presented in [17] is based on 25 years old CDF search for pair production of unit-charged particles which leave the detector before decaying [18]. As mentioned in [19] DO clearly excluded 200 GeV leptogluons decaying within the detector. The twenty years old H1 search for e_8 has excluded the compositeness scale $\Lambda < 3 \text{ TeV}$ for $M_{e_8} \approx 100 \text{ GeV}$ and $\Lambda < 240 \text{ GeV}$ for $M_{e_8} \approx 250 \text{ GeV}$ [20, 21]. While the LEP experiments did not perform dedicated search for leptogluons, low limits for excited lepton masses, namely 103.2 GeV [17], certainly is valid for ℓ_8 , too. Finally, reconsideration of CMS results on leptoquark searches performed in [7] leads to the strongest current limit on the e_8 mass, $M_{e_8} > 1.2 - 1.3 \text{ TeV}$.

The advantage of ep colliders with sufficiently high center of mass (CM) energies is that e_8 is produced in resonance mode. Large Hadron electron Collider [22] (LHeC) is the highest center of mass energy ep collider proposal up to date. Unfortunately, approved option which assumes 60 GeV energy recovery linac for electron beam [23], will not give an opportunity to cover e_8 masses above 1.3 TeV [11]. For this reason, ep colliders with higher energies should be considered for resonant production of e_8 .

In this paper, we consider resonant production of e_8 at the FCC based ep colliders. Main parameters of these colliders are given in Section II. Phenomenology of e_8 is presented in Section III. In Section IV, signal and background analyses have been performed and discovery limits on e_8 mass are estimated. Compositeness scale matters are discussed in Section V. Finally we summarize our results in Section VI.

II. FCC BASED ep COLLIDERS

It is widely known that lepton-hadron collisions have been playing a crucial role in exploration of deep structure of matter. For example, electron scattering on atomic nuclei reveals structure of nucleons in Hofstadter experiment [24], quark parton model was originated from lepton-hadron collisions etc [25]. Investigation of extremely small x

but sufficiently high Q^2 will provide a basis for deeper understanding of the nature of strong interactions at all levels ranging from nucleus to partons. In addition, the results from lepton-hadron colliders are necessary for adequate interpretation of physics at possible future hadron colliders. Today, linac-ring type ep machines seem to be the most convenient way to TeV scale in lepton-hadron collisions; and it is also possible that in future, μp machines can also be considered depending on solutions of the principal issues of the $\mu^+\mu^-$ colliders.

FCC [26] is future 100 TeV CM energy pp collider proposed at CERN and supported by European Union within the Horizon 2020 Framework Programme for Research and Innovation. It includes also an electron-positron collider option at the same tunnel (TLEP), as well as ep collider options. Construction of future e^+e^- colliders and $\mu^+\mu^-$ colliders tangential to FCC will give opportunity to achieve highest CM energies in ep and μp collisions [27–29]. A possible configuration of FCC based lepton-hadron colliders is shown in Figure 1.

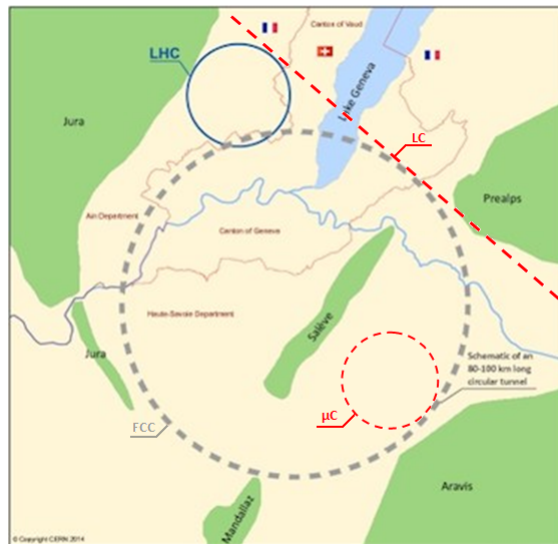


Figure 1. Possible configuration of FCC, linear collider (LC) and muon collider (μC).

CM energy and luminosity values for FCC based ep colliders - with three different options of electron beam energy - which we use in this study are given in Table II. In this table ERL60 denotes energy recovery linac proposed for LHeC, ILC means International Linear Collider [30] with highest energy and PWFA-LC denotes Plasma Wake-Field Accelerator Linear Collider [31] with highest energy (for details see refs. [27–29]). In principle, staged scheme can be considered for the FCC based ep colliders: starting from ERL60 \otimes FCC, through ILC \otimes FCC to the highest CM energy PWFA-LC \otimes FCC.

Table II. Main parameters of the FCC based ep colliders.

Collider Name	E_e , TeV	CM Energy, TeV	L_{int} , fb^{-1} per year
ERL60 \otimes FCC	0.06	3.46	100
ILC \otimes FCC	0.5	10	10-100
PWFA-LC \otimes FCC	5	31.6	1-10

III. COLOR OCTET ELECTRON

In fermion-scalar models with colored preons, leptons are bound states of one fermionic color triplet preon and one scalar color triplet anti-preon

$$\ell = (F\bar{S}) = 3 \otimes \bar{3} = 1 \oplus 8 \quad (1)$$

therefore, each SM lepton has one color octet partner. In three-fermion models with color triplet fermionic preons the color decomposition is

$$\ell = (FFF) = 3 \otimes 3 \otimes 3 = 1 \oplus 8 \oplus 8 \oplus 10 \quad (2)$$

and each SM lepton has two color octet and one color decuplet partners. Concerning the relation between compositeness scale and masses of leptogluons, two scenarios can be considered: $M_{e_8} \approx \Lambda$ (QCD-like scenario) and $M_{e_8} \ll \Lambda$ (Higgs-like scenario). In the second scenario SM-like hierarchy may be realized, namely, $M_{e_8} \ll M_{\mu_8} \ll M_{\tau_8} \ll \Lambda$. Interaction lagrangian of ℓ_8 with leptons and gluons can be written as [11, 17]

$$L = \frac{1}{2\Lambda} \sum_l \{ \bar{\ell}_8^\alpha g_s G_{\mu\nu}^\alpha \sigma^{\mu\nu} (\eta_L \ell_L + \eta_R \ell_R) + h.c. \}, \quad (3)$$

where g_s is strong coupling constant, Λ denotes compositeness scale, $G_{\mu\nu}$ is gluon field strength tensor, $\ell_{L(R)}$ stands for left (right) spinor components of lepton, $\ell = e, \mu, \tau$; $\sigma^{\mu\nu}$ is the antisymmetric tensor ($\sigma^{\mu\nu} = \frac{i}{2} [\gamma^\mu, \gamma^\nu]$), $\eta_L(\eta_R)$ symbolizes chirality factor. Keeping in mind leptonic chiral invariance ($\eta_L \eta_R = 0$), we take $\eta_L = 1$ and $\eta_R = 0$. Decay width of ℓ_8 given by

$$\Gamma(\ell_8 \rightarrow \ell + g) = \frac{\alpha_s M_{\ell_8}^3}{4\Lambda^2}, \quad (4)$$

where $\alpha_s = g_s/4\pi$. The decay width of e_8 is presented in Fig. 2 for $\Lambda = M_{e_8}$ and $\Lambda = 100$ TeV.

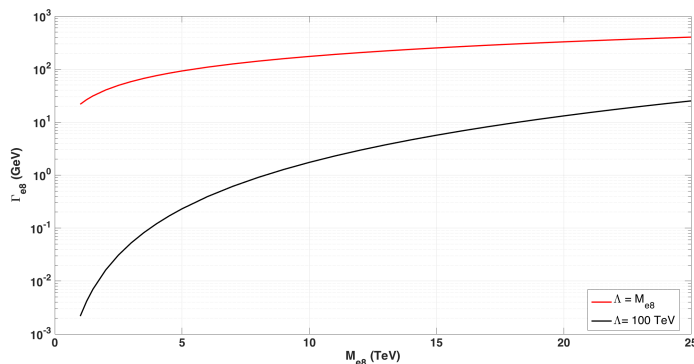


Figure 2. e_8 decay width vs its mass for $\Lambda = M_{e_8}$ and $\Lambda = 100$ TeV.

Diagram for resonant production of e_8 is shown in Figure 3. We implement model files of e_8 into MadGraph5 event generator [32] and use CTEQ6L1 parton distribution function [33] for numerical calculations. MadGraph5-Pythia6 interface was used for parton showering and hadronization [34].

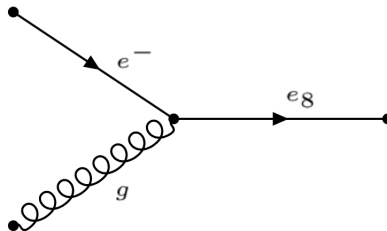


Figure 3. Feynman Diagram for resonant production of e_8 in ep collisions.

The resonant e_8 production cross sections for different options of the FCC based ep colliders (Table II) are presented in Fig. 4 (for $\Lambda = M_{e_8}$ and $\Lambda = 100$ TeV cases).

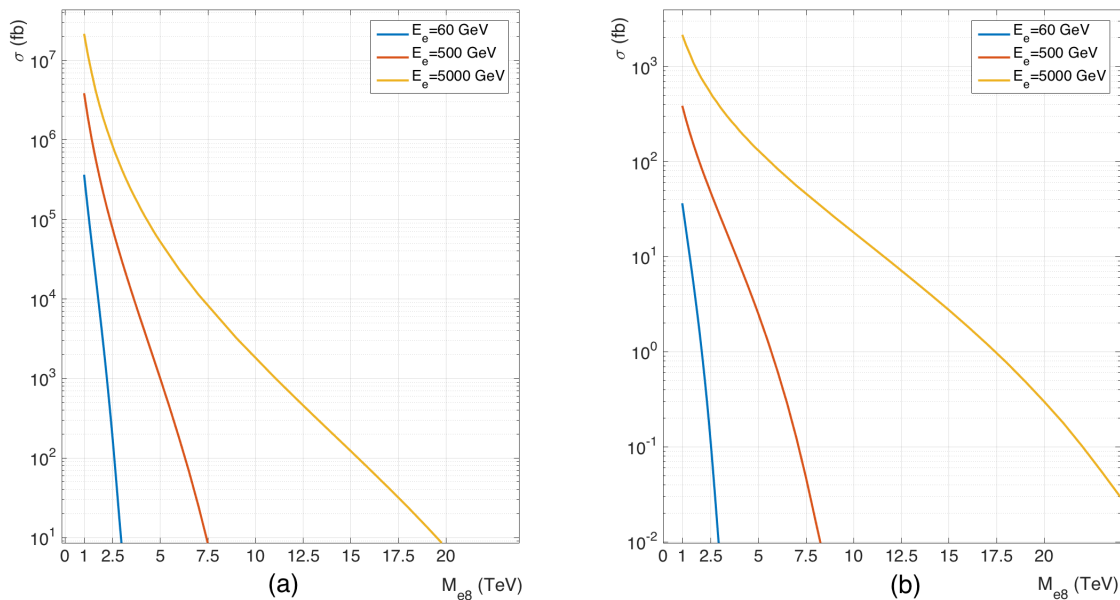


Figure 4. Resonant production of e_8 at the FCC based ep colliders for $\Lambda = M_{e_8}$ (a) and $\Lambda = 100$ TeV (b).

In order to emphasize the advantage of the resonant production let us compare the production of e_8 with mass 10 TeV at PWFA-LC \otimes FCC ($\sqrt{s_{ep}} = 31.6$ TeV, $L_{int} = 10$ fb^{-1}) and FCC-pp option ($\sqrt{s_{pp}} = 100$ TeV, $L_{int} = 500$ fb^{-1}). As seen from Fig. 4, production cross section at ep is 2000 fb for $\Lambda = 10$ TeV and 20 fb for $\Lambda = 100$ TeV, whereas corresponding cross sections for pair production of e_8 at the FCC-pp are ~ 0.50 fb and 0.29 fb , respectively. Therefore, numbers of produced e_8 are $n = 20000$ at ep and $n = 250$ at pp if $\Lambda = 10$ TeV. Corresponding numbers for $\Lambda = 100$ TeV are $n = 200$ and $n = 188$, respectively. Keeping in mind that ep collisions have more clear experimental environment than pp collisions, PWFA-LC \otimes FCC seems to be more advantageous even for $\Lambda = 100$ TeV case.

IV. SIGNAL - BACKGROUND ANALYSIS

In this section numerical calculations will be performed for $\Lambda = M_{e_8}$. In order to determine appropriate kinematical cuts p_T and η distributions for signal and background processes are computed. At this stage, generic cuts on electron and jet transverse momentum are chosen as $p_{T_e} = 20$ GeV and $p_{T_j} = 30$ GeV, respectively. Let us mention that jet corresponds to gluon for signal ($eg \rightarrow e_8 \rightarrow eg$ at partonic level) and quarks for main background ($eq \rightarrow eq$ through γ and Z exchanges) processes. Then discovery cuts on p_T and η are determined for different electron beam energy values and the invariant mass distributions are presented with these cuts. Finally, discovery limits on the color octet electron are presented.

Let us start with ERL60 \otimes FCC. Transverse momentum distribution of final state electrons (the same as for jets) is presented in Figure 5a. Keeping in mind that $M_{e_8} < 1.3$ TeV is excluded by the reconsideration of CMS results on leptoquark search [6], discovery cut $p_T > 500$ GeV seems to be adequate. Pseudorapidity distributions for electron and jets are shown in Figures 5b and 5c, respectively. As can be seen from Figure 5b, $\eta_e > 0.5$ cut drastically reduces the background while keeping the signal almost unaffected. In similar manner, $\eta_j > 2.1$ is chosen. Upper limit for both η_e and η_j is taken as $\eta_e, \eta_j < 4.74$ which corresponds to 1° in proton direction. This value can be covered by very forward detector as in the LHeC case [22]. Invariant mass distributions with generic cuts and discovery cuts are presented in Figures 5d and 6, respectively. It is seen that after discovery cuts, background goes down essentially below signal in the invariant mass distribution.

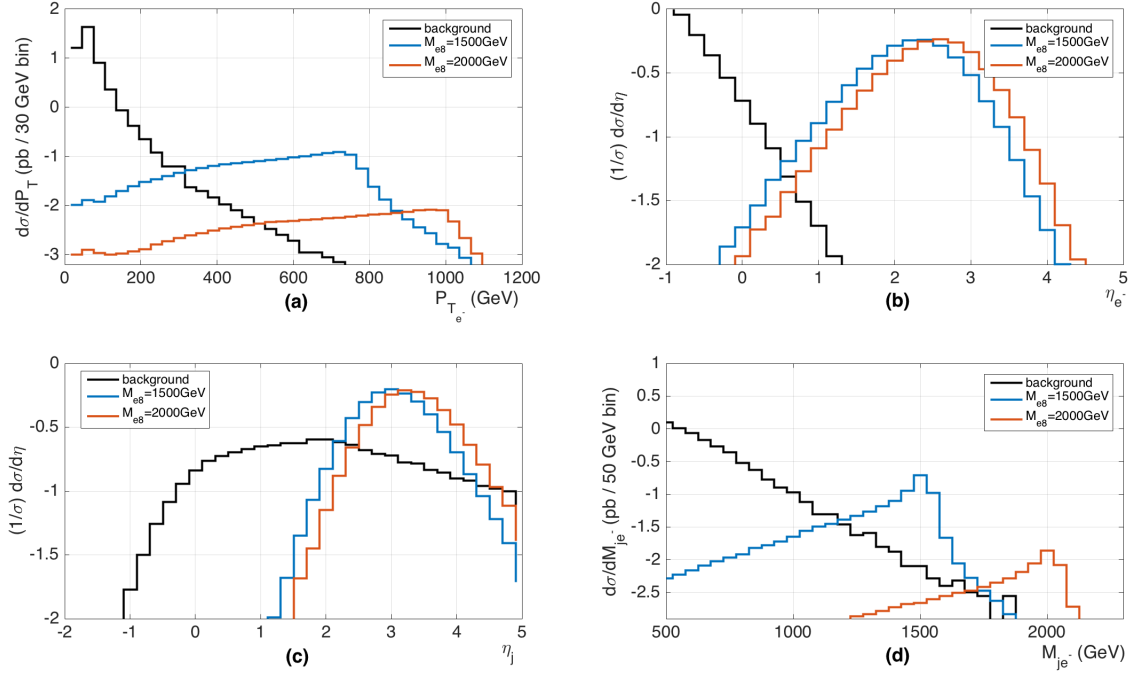


Figure 5. a) Transverse momentum distributions of final state jets (and electrons), b) pseudorapidity distributions of final state electrons, c) pseudorapidity distributions of final state jets and d) invariant mass distributions for signal and background at ERL60 \otimes FCC after generic cuts.

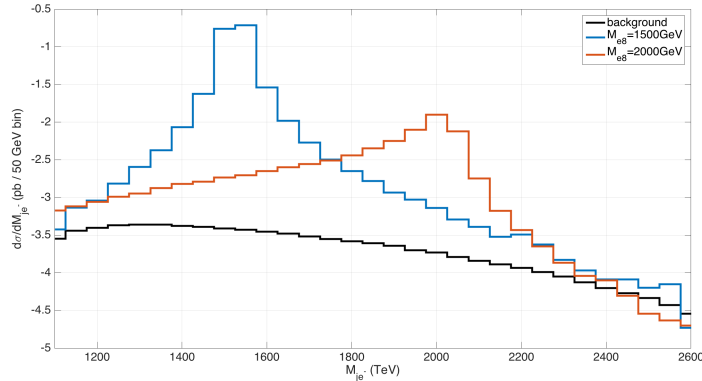


Figure 6. Invariant mass distributions for signal and background at ERL60 \otimes FCC after discovery cuts.

In order to determine discovery limits for color octet electron, we use following formula for statistical significance:

$$SS = \sqrt{2[(S + B) \ln(1 + (S/B)) - S]} \quad (5)$$

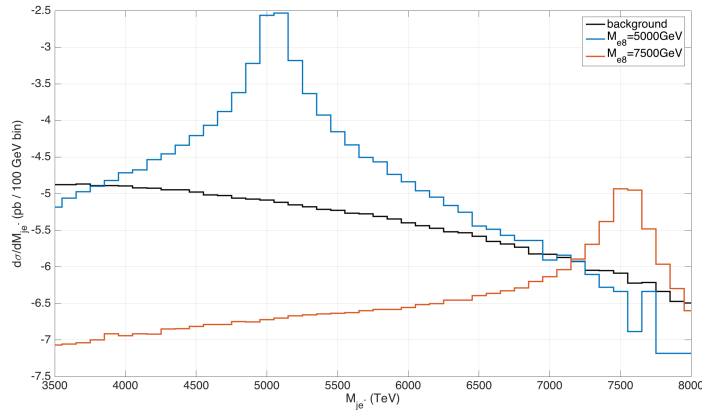
where S and B denote event numbers of signal and background, respectively. In addition to discovery cuts, mass window cuts are specified to determine S and B values as $M_{e_8} - 2\Gamma_{e_8} < M_{e_j} < M_{e_8} + 2\Gamma_{e_8}$. Discovery ($SS = 5$) and observation ($SS = 3$) limits for 100 fb^{-1} integrated luminosity are found to be 2900 and 3100 GeV, respectively.

Performing similar analysis for ILC \otimes FCC and assuming that e_8 is not observed by ERL60 \otimes FCC (that means $M_{e_8} > 3100 \text{ GeV}$) we determine following discovery cuts: $p_T > 1500 \text{ GeV}$, $-1.5 < \eta_e < 4.74$ and $0.5 < \eta_j < 4.74$. Invariant mass distributions after discovery cuts are presented in Fig. 7. Discovery limits for ILC \otimes FCC with 10 and 100 fb^{-1}

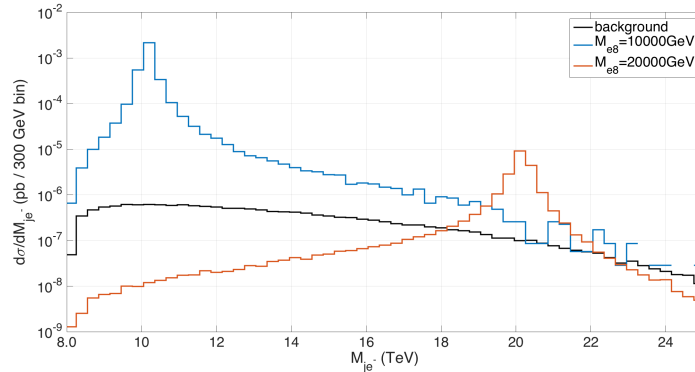
Table III. Observation (3σ) and discovery (5σ) limits for e_8 at different ep colliders.

Collider Name	L_{int}, fb^{-1}	M_{e_8}, TeV	
		3σ	5σ
ERL60 \otimes FCC	100	3.1	2.9
ILC \otimes FCC	10	8.4	8.1
	100	8.9	8.6
PWFA-LC \otimes FCC	1	21.6	20.1
	10	24.3	23.1

integrated luminosities are presented in Table III. Equation 5 and mass window $M_{e_8} - 2\Gamma_{e_8} < M_{e_j} < M_{e_8} + 2\Gamma_{e_8}$ have been used.

Figure 7. Invariant mass distributions for signal and background at ILC \otimes FCC after discovery cuts.

Similar consideration for PWFA-LC \otimes FCC results in following discovery cuts: $p_T > 4000$ GeV (assuming that e_8 is not observed at ILC \otimes FCC), $-2.9 < \eta_e < 4.74$ and $-1.0 < \eta_j < 4.74$. Invariant mass distributions after these cuts are presented in Fig. 8. Discovery limits for PWFA-LC \otimes FCC with 1 and 10 fb^{-1} integrated luminosities are presented in last two rows of Table III.

Figure 8. Invariant mass distributions for signal and background at PWFA-LC \otimes FCC after discovery cuts.

V. LIMITS ON COMPOSITENESS SCALE

If the e_8 is discovered by FCC-pp option, ep colliders will give opportunity to estimate compositeness scale. In this regard, two distinct possibilities should be considered:

- e_8 is discovered by FCC but not observed at e-FCC. In this case one can put lower limit on compositeness scale,

b) e_8 is discovered by FCC and also observed at e-FCC. In this case one can determine compositeness scale.

In this section we present the analysis of these two possibilities for four different benchmark points, namely, $M_{e_8} = 2.5, 5, 7.5$ and 10 TeV.

A. e_8 is discovered by FCC but not observed at e-FCC

Since the e_8 mass is known one can determine optimal cuts for given M_{e_8} . Let us start by consideration of $M_{e_8} = 2.5$ TeV at ILC \otimes FCC. It is seen from Fig. 5 that $p_T > 500$ GeV, $-1.30 < \eta_e < 4.74$, $0.50 < \eta_j < 3.00$ cuts drastically decrease the background whereas the signal is slightly affected. Similar analyses are performed for other collider options and M_{e_8} values. Optimal cuts are presented in Table V. Invariant mass window $0.99M_{e_8} < M_{e_j} < 1.01M_{e_8}$ has been used in this particular analysis.

Table IV. Optimal cuts for determination of compositeness scale lower bounds.

Collider	Cut Type	$M_{e_8} = 2.5$ TeV		$M_{e_8} = 5.0$ TeV		$M_{e_8} = 7.5$ TeV		$M_{e_8} = 10$ TeV	
		min	max	min	max	min	max	min	max
ERL60 \otimes FCC	η_e	0.6	4.74	-	-	-	-	-	-
	η_j	2.4	4.74	-	-	-	-	-	-
	Mass Window	2475	2525	-	-	-	-	-	-
ILC \otimes FCC	η_e	-1.3	4.74	-1.1	4.74	-0.8	4.74	-	-
	η_j	0.5	3.0	1.0	3.8	1.3	4.2	-	-
	Mass Window	2475	2525	4950	5050	7425	7575	-	-
PWFA-LC \otimes FCC	η_e	-3.3	4.74	-2.9	4.74	-2.7	4.74	-2.6	4.74
	η_j	-1.8	0.7	-1.2	1.7	-0.9	2.0	-0.6	2.4
	Mass Window	2475	2525	4950	5050	7425	7575	9900	10100

Applying cuts presented in Table V and $p_T > 500$ GeV for all cases one can estimate achievable lower limits on compositeness scale. Using Eq. 5 we obtain Λ values given in Table VI. As expected, lower bounds on compositeness scale is decreased with increasing value of the e_8 mass. It is seen that multi-hundred TeV lower bounds can be put on compositeness scale if e_8 is discovered at the FCC and not observed at ILC \otimes FCC and PWFA-LC \otimes FCC.

Table V. Lower limits on compositeness scale in TeV units at the FCC based ep colliders

Collider	L_{int}, fb^{-1}	$M_{e_8} = 2.5$ TeV		$M_{e_8} = 5.0$ TeV		$M_{e_8} = 7.5$ TeV		$M_{e_8} = 10$ TeV	
		3σ	5σ	3σ	5σ	3σ	5σ	3σ	5σ
ERL60 \otimes FCC	100	44	34	-	-	-	-	-	-
ILC \otimes FCC	10	250	195	75	58	22	15	-	-
	100	450	350	135	105	42	32	-	-
PWFA-LC \otimes FCC	1	220	170	200	150	190	145	110	80
	10	400	305	390	300	360	275	200	155

B. e_8 is discovered by FCC and observed at e-FCC

In this case, the value of cross section at ep colliders which is inversely proportional to Λ^2 gives opportunity to determine compositeness scale directly. As an example, let us consider ILC \otimes FCC case. In Fig. 9 we present Λ dependence of e_8 production cross section for $M_{e_8} = 2.5, 5, 7.5$ TeV. Supposing that FCC discovers e_8 with 5 TeV mass and e-FCC measure cross section as $\sigma_{exp} \sim 2.50 fb$, one can derive compositeness scale as $\Lambda_{exp} = 100$ TeV.

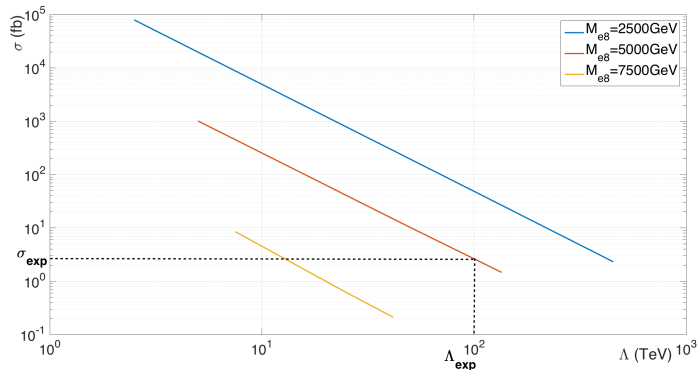


Figure 9. Cross section distributions with respect to compositeness scale for ILC \otimes FCC collider.

VI. CONCLUSION

It seems that FCC based ep colliders have great potential for e_8 searches. Discovery limits for e_8 at the LHC, FCC, ILC, PWFA-LC and FCC based ep colliders assuming $\Lambda = M_{e_8}$ are summarized in Figure 10. Discovery limit 2.5 TeV for LHC is taken from [6]. A discovery limit of 15 TeV for FCC is obtained by rescaling LHC limit using the procedure developed by G. Salam and A. Weiler [35]. It is clear that discovery limits for pair production of e_8 at lepton colliders are approximately $\sqrt{s}/2$. The search potential of ILC \otimes FCC essentially exceeds that of LHC and linear colliders whereas is lower than FCC. Highest potential for e_8 search will be provided by PWFA-LC \otimes FCC with discovery limit of 23 TeV which is higher than 15 TeV discovery limit provided by FCC pp collider. On the other hand, observation of e_8 at the FCC based ep colliders will provide an opportunity to determine compositeness scale, in some cases up to multi-hundred TeV. In addition, polarized e-beams will give opportunity to clarify Lorentz structure of $e_8 - e - g$ vertex (this subject is under consideration).

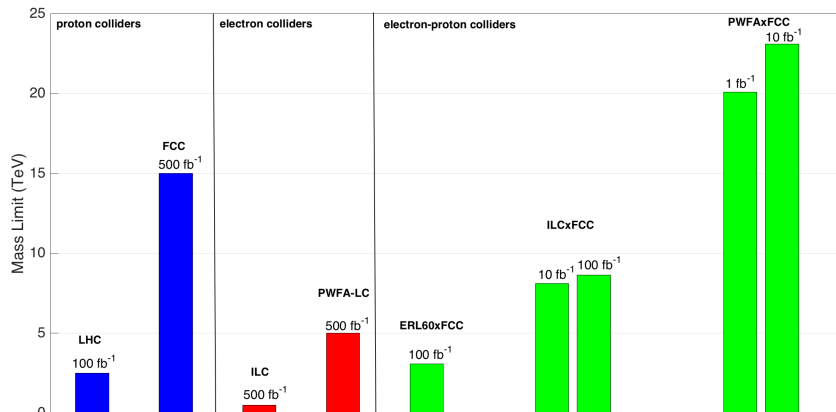


Figure 10. Discovery limits for e_8 at different pp, e^+e^- and ep colliders.

Finally, FCC based energy frontier ep colliders have great potential for BSM phenomena search, especially when related to the first SM family fermions. A similar statement is correct for FCC based μp colliders if BSM phenomena are related to the second SM family fermions. Therefore, ERL60 \otimes FCC should not be considered as the sole choice for the FCC based lp colliders. Energy frontier lp options should also be investigated at the same level. The proper choice for FCC based lp collider option will be determined by the FCC results.

ACKNOWLEDGMENTS

This study is supported by TUBITAK under the grant no 114F337. Authors are grateful to Gokhan Unel and Frank Zimmermann for useful discussions. Authors are also grateful to Subhadip Mitra and Tanumoy Mandal for sharing leptogluon MadGraph model file.

-
- [1] ATLAS Collaboration, “Observation of a new particle in the search for the Standard Model Higgs boson with the ATLAS detector at the LHC”, *Phys. Lett. B* 716 (2012) 1, doi:10.1016/j.physletb.2012.08.020, arXiv:1207.7214.
- [2] CMS Collaboration, “Observation of a new boson at a mass of 125 GeV with the CMS experiment at the LHC”, *Phys. Lett. B* 716 (2012) 30, doi:10.1016/j.physletb.2012.08.021, arXiv:1207.7235.
- [3] J. C. Pati and A. Salam, *Phys. Rev. D* 10, 275 (1974) [*Phys. Rev. D* 11, 703 (1975)].
- [4] I. A. D’ Souza, C. S. Kalman, PREONS: Models of Leptons, Quarks and Gauge Bosons as Composite Objects, World Scientific Publishing Co. (1992).
- [5] A. Celikel, M. Kantar and S. Sultansoy, “A search for sextet quarks and leptogluons at the LHC”, *Phys. Lett. B* 443 (1998) 359.
- [6] T. Mandal and S. Mitra, “Probing color octet electrons at the LHC”, *Phys. Rev. D* 87 (2013) 095008.
- [7] D. Gonçalves-Netto et al., “Looking for leptogluons”, *Phys. Rev. D* 87 (2013) 094023.
- [8] T. Jelinski and D. Zhuridov, “Leptogluons in dilepton production at LHC”, e-Print:arXiv:1510.04872 [hep-ph].
- [9] T. Mandal, S. Mitra, and S. Seth. “Probing compositeness with the CMS eej & eej data” *Physics Letters B* 758 (2016): 219-225. arXiv:1602.01273v1
- [10] A. Celikel and M. Kantar, “Resonance Production of New Resonances at ep and γp Colliders”, *Tr. J. of Physics* 22 (1998) 401.
- [11] M. Sahin, S. Sultansoy and S. Turkoz, “Resonant production of color octet electron at the LHeC”, *Phys. Lett. B* 689 (2010) 172.
- [12] M. Sahin, “Resonant production of spin-3/2 color octet electron at the LHeC”, *Acta Physica Polonica B* 45 (2014) 1811.
- [13] K. Cheung, “Muon-proton colliders: Leptoquarks, contact interactions and extra dimensions”, *AIP Conference Proceedings* 542 (2000) 160.
- [14] A. N. Akay, H. Karadeniz, M. Sahin and S. Sultansoy, “Indirect search for color octet electron at next-generation linear colliders”, *EPL* 95 (2011) 31001.
- [15] IceCube Collab. (M. G. Aartsen et al.), *Phys. Rev. Lett.* 113, 101101 (2014), arXiv:1405.5303 [astroph.HE].
- [16] A. N. Akay et al., “New IceCube data and color octet neutrino interpretation of the PeV energy events”, *Int. J. Mod. Phys. A* 30 (2015) 1550163.
- [17] K. A. Olive et al. (Particle Data Group), *Chin. Phys. C* 38 (2014) 090001.
- [18] F. Abe et al. (CDF Collaboration), “Search for Heavy Stable Charged Particles in 1.8-TeV pp(bar) collisions at the Fermilab Collider”, *Phys. Rev. Lett.* 63 (1989) 1447. 15
- [19] J. L. Hewett and T.G. Rizzo, “Much ado about leptoquarks: A comprehensive analysis”, *Phys. Rev. D* 56 (1997) 5709.
- [20] I. Abt et al. (H1 Collaboration), “A search for leptoquarks, leptogluons and excited leptons in H1 at HERA”, *Nucl. Phys. B* 396 (1993) 3.
- [21] T. Ahmed et al. (H1 Collaboration), “A search for leptoquarks and squarks at HERA”, *Z. Phys. C* 64 (1994) 545.
- [22] J. L. Abelleira Fernandez et al. (LHeC Study Group), “A Large Hadron Electron Collider at CERN: Report on the Physics and Design Concepts for Machine and Detector”, *J. Phys. G: Nucl. Part. Phys.* 39, 075001 (2012).
- [23] LHeC web page: <http://lhec.web.cern.ch/erl-facility>
- [24] R. Hofstadter and R. W. McAllister, *Phys. Rev.* 98, 217 (1955).
- [25] J. I. Friedman and H. W. Kendall, *Ann. Rev. Nucl. Sci.* 2, 203 (1972); See also the published versions of the Nobel lectures: R. E. Taylor, *Rev. Mod. Phys.* 6, 573 (1991); H. W. Kendall, *Rev. Mod. Phys.* 6, 597 (1991); J. I. Friedman, *Rev. Mod. Phys.* 6, 615 (1991).
- [26] FCC web page: <https://fcc.web.cern.ch>.
- [27] Y. C. Acar, U. Kaya, B. B. Oner and S. Sultansoy, “FCC based ep and μp colliders”, arXiv:1510.08284 [hep-ex].
- [28] Y. C. Acar, U. Kaya, B. B. Oner and S. Sultansoy, “Main Parameters of LCxFCC Based Electron-Proton Colliders”, arXiv:1602.03089 [hep-ex].
- [29] S. Sultansoy, “FCC Based Lepton-Hadron and Photon-Hadron Colliders: Luminosity and Physics”, FCC Week 2016, Rome, Italy.
- [30] C. Adolphsen et al., The International Linear Collider Technical Design Report-Volume 3. II; arXiv:1306.6328.
- [31] J-P. Delahaye et al., A Beam Driven Plasma-Wakefield Linear Collider from Higgs Factory to Multi-TeV, in Proceedings of the Fifth International Particle Accelerator Conference, 2014 (Dresden, Germany), p. 3791.
- [32] J. Alwall, M. Herquet, F. Maltoni, O. Mattelaer and T. Stelzer, *JHEP* 1106, 128 (2011); arXiv:1106.0522 [hep-ph].
- [33] D. Stump et al., “Inclusive jet production, parton distributions and the search for new physics”, *JHEP* 0310 (2003) 046.
- [34] T. Sjostrand, S. Mrenna, and P. Z. Skands, “PYTHIA 6.4 physics and manual,” *JHEP* 0605 (2006) 026, arXiv:hep-ph/0603175 [hep-ph].
- [35] G. Salam and A. Weiler, “The Collider Reach project”, <http://collider-reach.web.cern.ch/collider-reach>.